Reconciling Discrepancies in the Observed Growth of Wind-generated Waves

KIMMO K. KAHMA

Finnish Institute of Marine Research, Helsinki, Finland

CHARLES J. CALKOEN

Delft Hydraulics Laboratory, Emmeloord, The Netherlands

(Manuscript received 6 May 1991, in final form 18 December 1991)

ABSTRACT

Spectra from various wave-growth experiments have been collected into a database, and the data have been reanalyzed to explain the differences in the observed growth rates.

For one of the experiments (Joint North Sea Wave Project: JONSWAP), the extensive wind data allowed the authors to perform a detailed analysis of the time history of the wind at a point moving with the group velocity of the peak of the wave spectrum. Using the average of the wind speed at this moving point, removing spectra that according to this wind estimate were not measured in steady or increasing wind, and taking into account the atmospheric stratification, the previously large discrepancy in the growth rates between JONSWAP and two other experiments (Bothnian Sea, Lake Ontario) was removed.

The analysis revealed significant differences between the spectra in different groups. Peak enhancement was higher in the Bothnian Sea data than in the other datasets at the same dimensionless fetch. Equally high peak enhancement could be found in the Lake Ontario data only at fetches an order of magnitude shorter. The averages of dimensionless frequency spectra in the saturation range were not consistent in different datasets, but the "grand average" of all the datasets showed the transition in the power law of the spectrum from -4 to -5.

1. Introduction

The best-controlled conditions for studying the evolution of the wave spectrum occur in steady wind when the fetch is limited by a straight shoreline orthogonal to the wind direction. In these conditions the Kitaigorodskii similarity law (Kitaigorodskii 1962) has been traditionally used to express the wave growth using the following dimensionless wave parameters:

dimensionless fetch

$$\tilde{X} = gX/U_{10}^2, \quad X^* = gX/u_*^2$$

dimensionless energy

$$\tilde{\epsilon} = g^2\epsilon/U_{10}^4, \quad \epsilon^* = g^2\epsilon/u_*^4$$

dimensionless peak frequency

$$\tilde{\omega}_p = \omega_p U_{10}/g, \; \omega_p^* = \omega_p u_*/g.$$

Here X is the fetch, $\epsilon = \int_0^\infty S(\omega)d\omega$ is the total variance of the spectrum and ω_p is the angular frequency of the peak of the spectrum. Both U_{10} (the wind speed at 10-m height) and u_* (the friction velocity) have been widely used as the scaling wind.

During field experiments, the actual conditions even in this best-controlled situation are seldom ideal, and usually the results show considerable scatter. As more experiments have been made, systematic differences have also become evident in the relations describing wave growth. Perhaps the most striking example (Fig. 1) is the difference between the growth relations deduced from the Joint North Sea Wave Project (JONSWAP) experiment (Hasselmann et al. 1973) and the Bothnian Sea data (Kahma 1981a), the latter showing double energy compared with the former. High energies were also found in the dataset that was used to calibrate the parametric GONO (Golven Noordzee) model (Janssen et al. 1984).

In 1979 a group of wave researchers started the Sea Wave Modeling Project (The SWAMP Group 1985) to intercompare the results of ten different wave models under a number of standardized test conditions. One of these conditions considered a simple fetch- and duration-limited growth case, with a uniform wind field perpendicular to the shoreline. For this case, growth curves were computed: energy and peak frequency versus fetch. The differences between the growth curves computed with different models turned out to be considerable (see Fig. 2). This was especially striking since all models had been calibrated against measured data. It is also revealing that the largest differences in the SWAMP comparison were about the same size as the

Corresponding author address: Dr. Kimmo K. Kahma, Finnish Institute of Marine Research, P.O. Box 33 SF-00931, Helsinki, Finland.

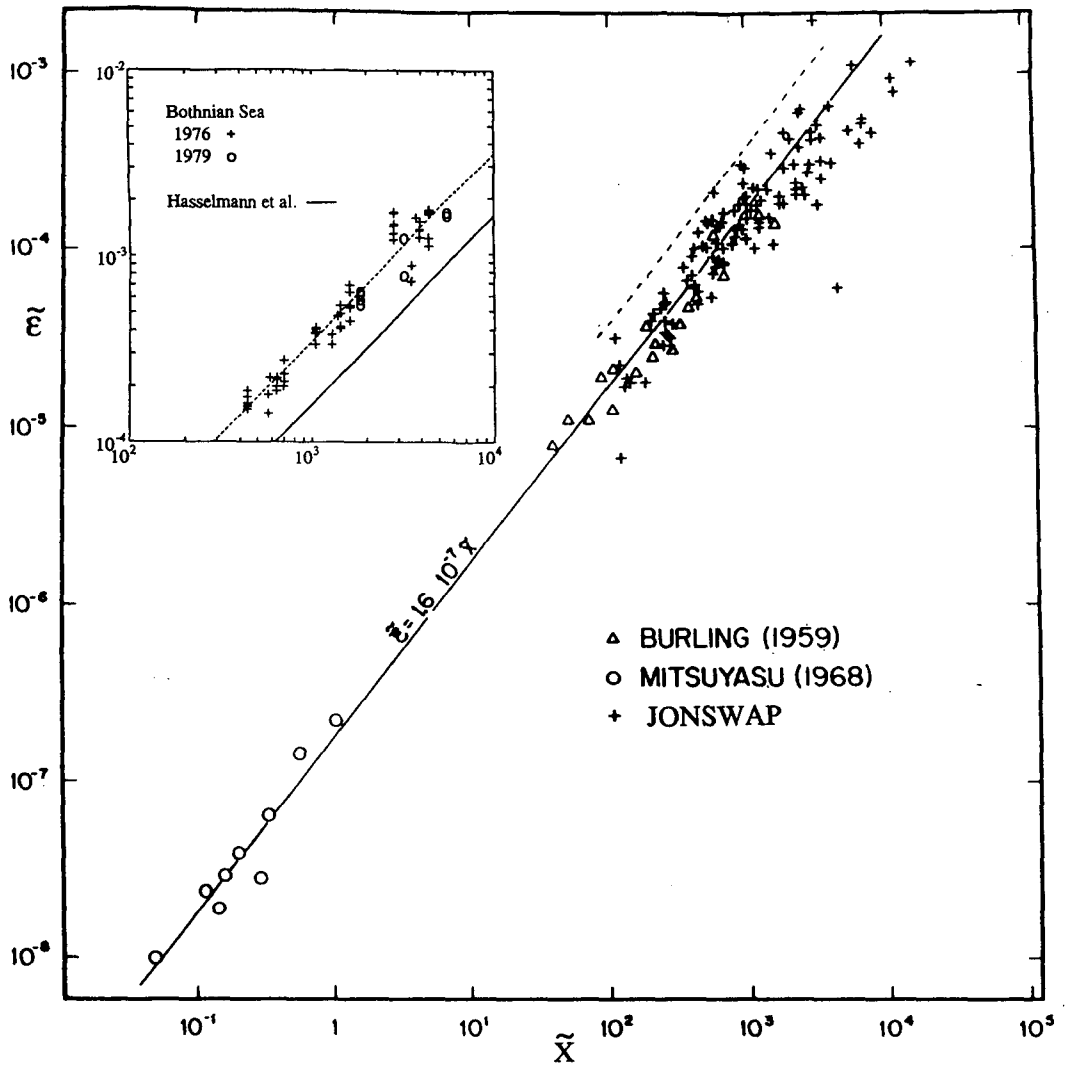

FIG. 1. An illustration of the differences in the empirical grow relations: the relations $\tilde{\varepsilon} = 1.6 \cdot 10^{-7} \tilde{X}$ (solid line), reported in Hasselmann et al. (1973), and $\tilde{\varepsilon} = 3.5 \cdot 10^{-7} \tilde{X}$ (dashed), found in the Bothnian Sea experiments of 1976 and 1979 (Kahma 1981a), are plotted on the data in Fig. 2.10 of Hasselmann et al. (1973). In the inset the same relations are plotted on the Bothnian Sea data.

difference between the Bothnian Sea data (Kahma 1981a) and the JONSWAP relations (Hasselmann et al. 1973).

One of the recommendations of the SWAMP Group for this test case was that existing experimental datasets should be collected in a database, which could subsequently be reanalyzed. A uniform reanalysis could clarify the discrepancies between the results of the computer models and give insight into other physical mechanisms that influence wave growth, such as atmospheric stability, the gustiness of the wind, the background wave field, fetch geometry, and wave–current interactions. In the framework of the WAM (wave modeling) project the aforementioned recommendation of the SWAMP Group has been carried out as a WAM subtask. It was initiated by Gerbrand Komen as chairman of the WAM project and Willem J. P. de Woogt as chairman of the subtask. The results of this work have been reported in the VII and VIII WAM meetings in 1989 and 1990.

A uniform analysis using a smaller database (Kahma 1986) was not able to find any single factor that alone could explain the observed differences in the growth curves. This is also the result of our present analysis. We were, however, able to identify two factors: stability and the variability of the wind, which gave a consistent explanation of the differences among the Bothnian Sea data, the JONSWAP data, and the Lake Ontario data.

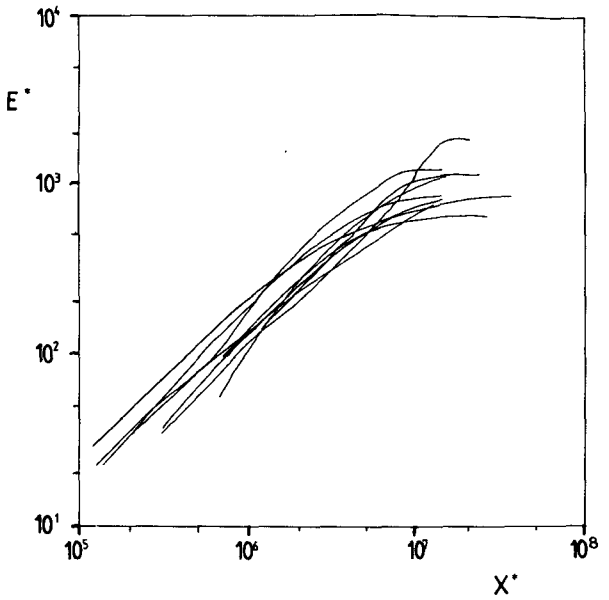

FIG. 2. Fetch-limited growth curves, SWAMP case II.

The important question of whether true friction velocity u_* is a better scaling wind speed than U_{10} could not be settled in this study because data about the true friction velocity was not available. It was found out, however, that when u_* was calculated by the widely used wind-dependent drag coefficient and the stability was taken into account by the Monin–Obukhov similarity theory, the scatter was not reduced much and the improvement was related only to the atmospheric stability.

2. The WAM database

The database, as it was used in this study, consists of the following experiments:

- Queen Elizabeth II Reservoir (Birch and Ewing 1986)
- Lake Ontario (Donelan et al. 1985)
- JONSWAP (Hasselmann et al. 1973; the subset for orthogonal fetch as selected by Müller 1976)
- Bothnian Sea (Kahma 1981a,b)
- ARSLOE (Rottier and Vincent 1982)
- Lake Marken (Bouws 1986)

No temperature data were available from the second half of the JONSWAP experiment.

The data of the Lake Marken experiment have been added to the database at a later stage. These data have not been used in the analysis of the growth curves (section 4) because the shallowness of Lake Marken prohibits a direct comparison with the other datasets.

3. The spectra

a. Individual spectra

Figure 3 shows representative examples of the energy spectra of all experiments contained in the database. Inspection of the spectra reveals clear differences in their form, energy scale, and frequency range. The Bothnian Sea data and the data from Queen Elizabeth II Reservoir have pronounced peaks with little other structure. The spectra from Lake Ontario seem generally to belong to the same category, but because a much wider frequency band has been used to average the data, both the peakiness and the steepness of the forward phase of the spectrum are slightly altered. Many of the spectra from the JONSWAP experiment show more structure, and a pronounced swell is present in the ARSLOE spectra.

The Bothnian Sea spectra stand out from the rest by having a larger peak enhancement than any other experiment at similar dimensionless fetches. The Lake Ontario data have comparable peak enhancements at fetches an order of magnitude shorter. Here we mean by peak enhancement the ratio of the spectrum at the peak and the extrapolation using the power law in the high-frequency part.

Before the spectra can be compared at high frequencies, it must be taken into account that the highest reliable frequency is not the same for different datasets, and that it usually falls well below the Nyquist frequency. To make the data as uniform as possible, we estimated the highest reliable frequency for each instrument. We took into account, for example, the response of a buoy, or the reflections from the supporting poles in the case of a wave staff. Aliasing was also calculated, because most of the experiments had taken advantage of the steep rear phase of the spectrum and had not used any antialiasing filter. The highest reliable frequency was then stored in the database, and spectral estimates above it were not used in the following dimensionless comparisons.

Figure 4 shows the same spectra as Fig. 3. Here the dimensionless spectrum

$$\tilde{S} = S\omega^5/g^2$$

is plotted versus $\tilde{\omega} = \omega U_{10}/g$ ($\omega = 2\pi f$). This transformation of the spectrum is particularly revealing for the form of the tail. If the spectrum has a ω^{-5} tail, $\tilde{S}$ is constant and equivalent to the so-called Phillips constant. In this form, conspicuous differences are again seen in the form of the spectra obtained in different experiments. Figure 4 shows typical ω^{-4} tails in the Bothnian Sea and JONSWAP experiments and ω^{-5} tails in the Queen Elizabeth II Reservoir experiment. With some imagination, one could see a transition of a ω^{-4} into a ω^{-5} tail in the last Lake Marken spectrum.

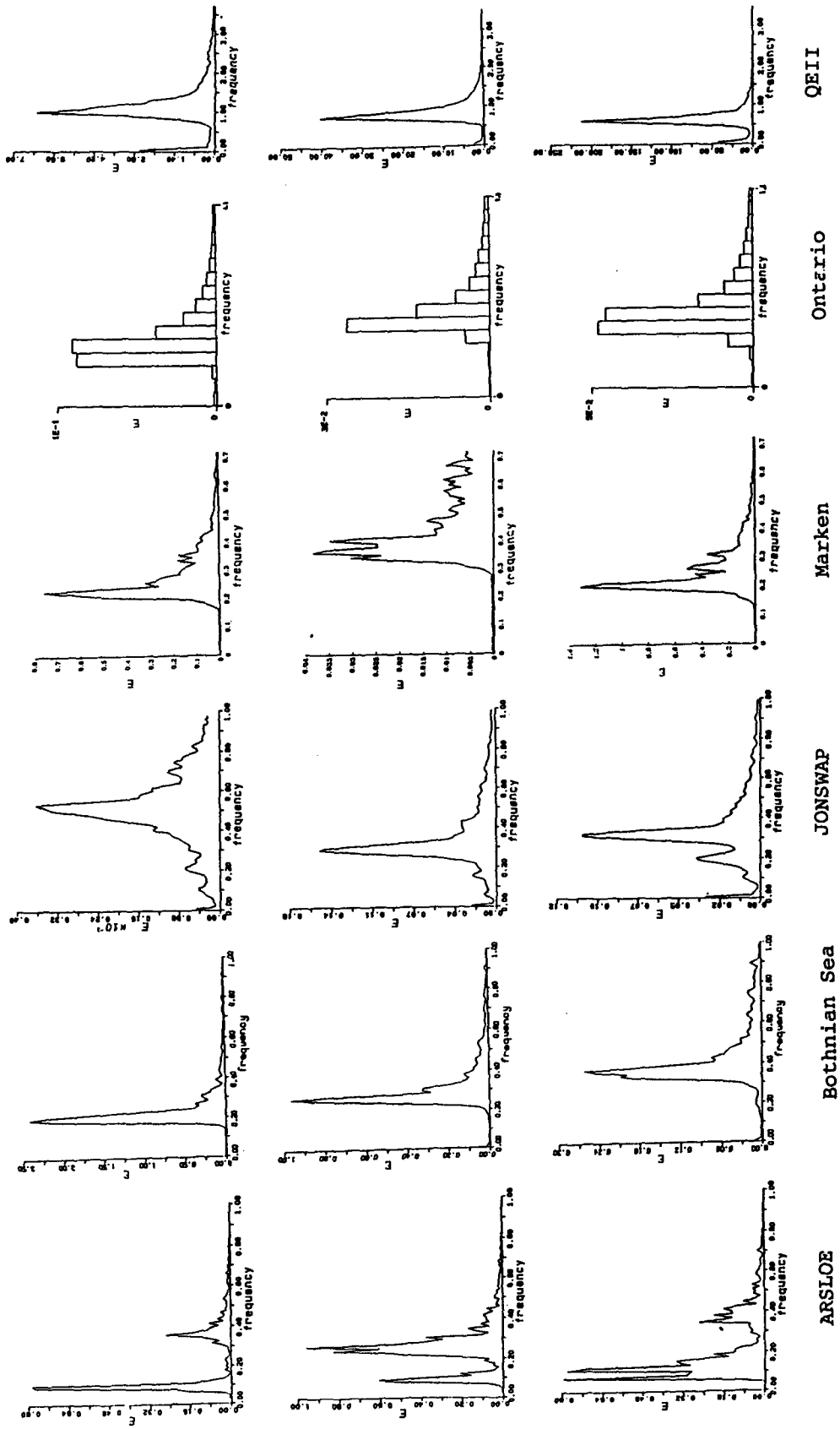

FIG. 3. Examples of energy spectra.

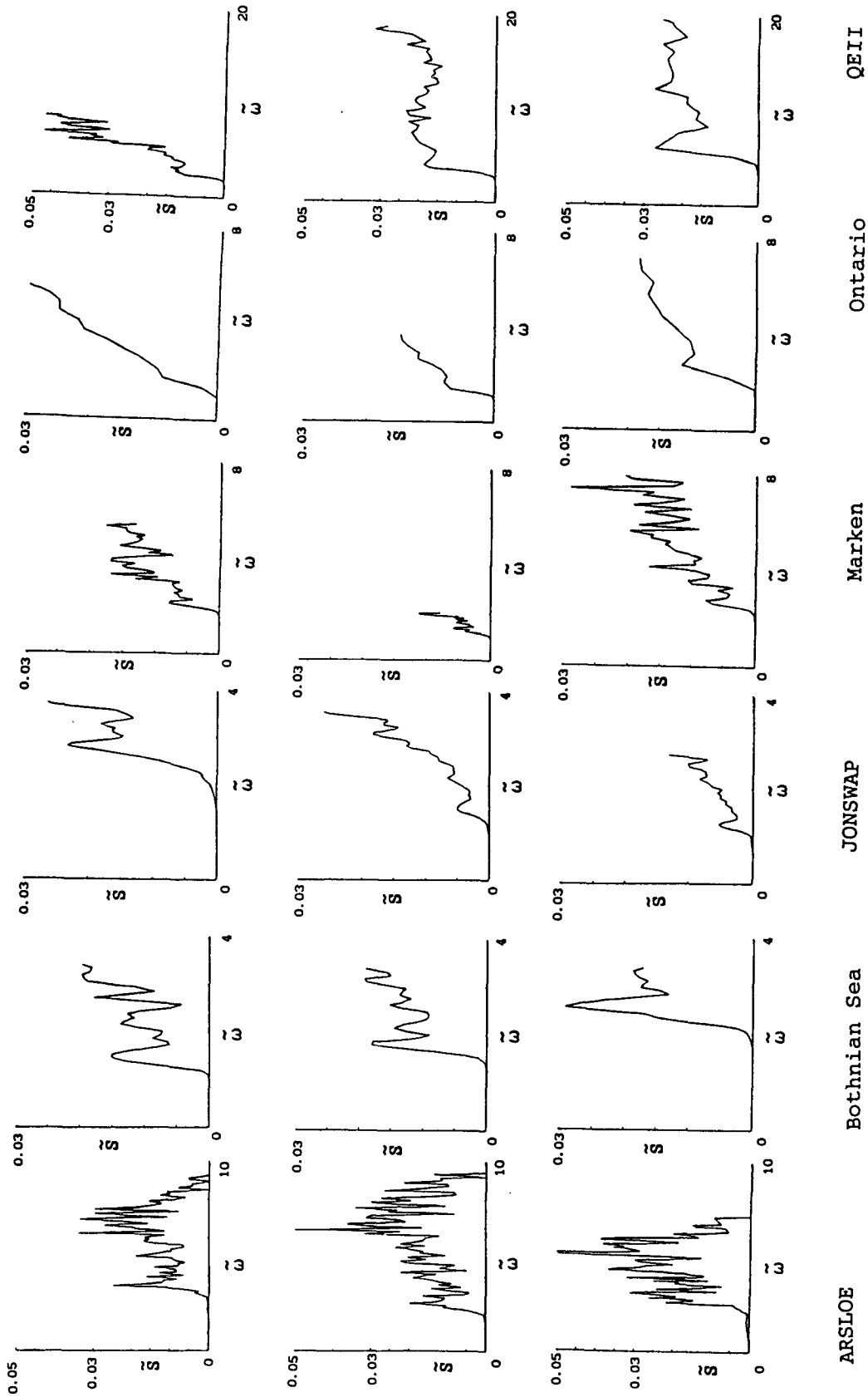

FIG. 4. The spectra of Fig. 3 in dimensionless form.

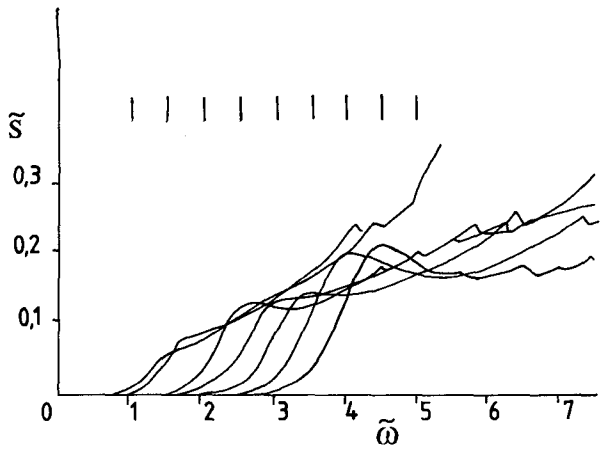

FIG. 5. Averaged dimensionless spectra from Lake Ontario.

b. Averaged dimensionless spectra

Individual spectra show a considerable scatter in the values of single-energy bins, which prevents one from drawing reliable conclusions. If the scaling law is valid, the dimensionless spectrum at a fixed dimensionless fetch should be constant. This makes it possible to average spectra, showing statistical properties more clearly. Figure 5 shows averaged dimensionless spectra from the Lake Ontario experiment, grouped by the dimensionless peak frequency.

While the spectra in Fig. 5 suggest that the saturation range is fetch dependent, the JONSWAP and the Bothnian Sea spectra do not show that feature (see Kahma 1981a,b). Because Lake Ontario data were measured in a single place, the fetch variations come from the change of wind speed and direction. It is therefore possible, in principle, that factors altering the saturation range are in this case correlated with the fetch. If this is the case and the saturation range at fixed external conditions indeed is independent of fetch, all the tails of dimensionless spectra can be averaged. Figure 6 shows the averaged tails for all the experiments in the database. To compute this plot, from each spectrum the part with frequencies higher than 1.2 times the peak frequency was used. The next step was to make a "grand-average tail," in which the averaged tail functions of the various experiments were combined in one plot. Figure 7 shows the grand-averaged spectral tail combining all the experiments in the database except the Lake Marken set, plus the averaged tails for the Lake Marken set alone.

It is interesting to see that this grand average shows the transition from a ω^{-4} to a ω^{-5} tail in the neighborhood of $\tilde{\omega} = 5$, as previously reported by Forristall (1981) and Kahma (1981a,b), and proposed on a theoretical basis by Kitaigorodskii (1983). Neither the individual spectra nor all the different group averages, however, seem to obey this form. It seems that the frequency spectrum does not have a universal form in the saturation range.

It is possible that the wavenumber spectrum has a universal shape showing the transition from ω^{-4} to ω^{-5}, and that deviations come from directional effects: the Doppler shift induced by currents and the orbital velocities of the waves near the peak of the spectrum. But the analysis supports equally well the possibility that the transition in the grand average is a climatological consequence of the various physical factors controlling the saturation range. In any case, the dimensionless frequency about 5 seems to be important in the statistical analysis of wave growth.

4. The growth curves

a. The scaling wind speed

The Kitaigorodskii similarity law (Kitaigorodskii 1962) uses U_∞, the wind speed at the upper boundary of the surface boundary layer. This can be determined only if the vertical structure of the boundary layer is known. In practice, U_∞ has to be replaced by some measured variable. It is still an open question whether the best variable to use is the friction velocity u_*, as Kitaigorodskii originally suggested; U_{10}; or maybe some other parameter such as the wind at the height $\lambda/2$, as proposed by Donelan and Pierson (1987). This study has used both U_{10} and u_*.

The main problem with the friction velocity is that no direct measurements are available for the experiments in the WAM database. In fact, we have not encountered any study in which an actual measurement of the friction velocity has been used in the scaling law. This study has used, in the case of neutral stratification, the wind-dependent drag coefficient:

$$C_D = 0.8\ 10^{-3} + 0.065 \times 10^{-3} U_{10}. \qquad (1)$$

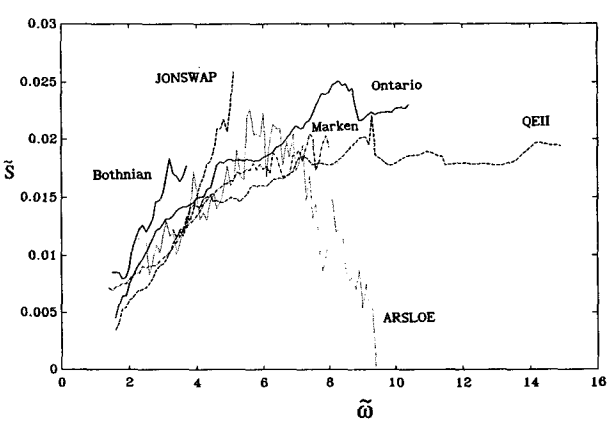

FIG. 6. Averaged dimensionless spectra in the saturation range: frequencies below $1.2\omega_p$ have been excluded from each spectrum.

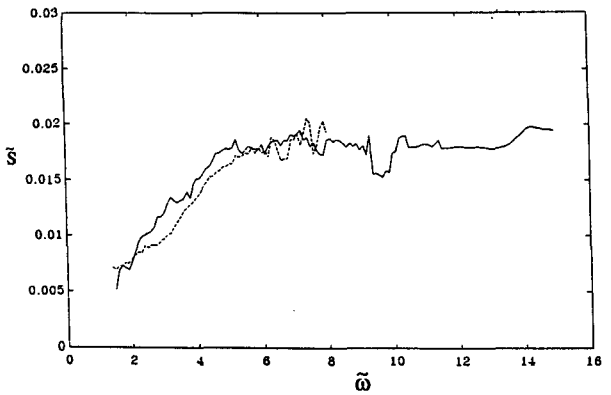

FIG. 7. "Grand average" of the dimensionless spectra in the saturation range. Lake Marken data (the dashed line) is shown separately because it represents shallow-water conditions.

This drag coefficient gives essentially the same results as the Charnock relation (Charnock 1955), and it has been used, for example, by Janssen et al. (1987) and by Bouws (1986) to show that scaling by u_* reduces scatter. When temperature data have been available, the effect of stability on u_* has been taken into account by using the Monin–Obukhov similarity theory (Monin and Yaglom 1971), which gives the velocity profile

$$U(z) = \frac{u_*}{\kappa}(\ln(z/z_0) - \Psi_M(z/L)).$$

Here κ is the von Kármán constant for which we have used the value 0.4, z_0 is the roughness length, L is the Monin–Obukhov stability length, and Ψ_M is the integrated universal function. For Ψ_M, the Businger–Dyer form was used with the parameters recommended by Lo and McBean (1978). The Monin–Obukhov stability parameter $\zeta = z/L$ was calculated, as usual, from the bulk Richardson number

$$R_b = \frac{g(T_a - T_w)/z_t}{T_a(U/z)^2}$$

by solving iteratively the equation

$$R_b = \zeta \frac{z}{z_t} \frac{\ln \frac{z_t}{z_H} - \Psi_H\left(\zeta \frac{z_t}{z}\right)}{\left[\ln \frac{z}{z_0} - \Psi_M(\zeta)\right]^2}.$$

Here z is the height of the wind measurement, z_t is the height of the temperature measurement, z_H is the roughness length for the temperature, and Ψ_H is the integrated universal function for the temperature. Since no better estimate was available, z_H was approximated by z_0.

b. *Spurious correlations*

Wind speed appears in all the dimensionless variables that are commonly used in growth analysis. It is well known that when such variables are correlated, spurious correlations may arise because both the function and the argument are functions of the same variable. If this common variable is inaccurate, and all other variables are nearly constant, the correlation between the dimensionless variables can be entirely spurious. On the other hand, when the variation of the variables is large, spurious correlation between the same variables may be of no importance. One cannot categorically say that dimensional analysis or certain dimensionless variables are unusable; the question has to be evaluated *in casu* for the data in question.

Several authors (e.g., Hasselmann et al. 1976; Donelan et al. 1985) have chosen the dimensionless peak frequency $\tilde{\omega}_p$ as the independent variable. Besides that the peak frequency is rather well defined and its statistical variability is fairly small, it has been argued that $\tilde{\omega}_p$ can be considered to be a local variable that describes the actual stage of development of the wave field even in variable wind.

From the point of view of spurious correlations, dimensionless peak frequency is not a very satisfactory variable. This can be seen from Table 1 in which the defining equations of the dimensionless variables have been factorized to reveal the spurious relations. Note that the physical relation between dimensionless energy and dimensionless peak frequency is so close to the spurious relation that extremely high accuracy is required to avoid at least some contamination from spurious correlation. This is even more so if $\tilde{\omega}_p$ is replaced by the inverse wave age U_c/c_p, proposed by Donelan et al. (1985). (Here $U_c = U\cos\theta$ is the component of the wind in the direction of travel of the waves at ω_p, and c_p is the phase speed of the waves at ω_p.) While the use of U_c/c_p instead of $\tilde{\omega}_p$ can be justified by physical arguments, and the properties of directional spectra strongly support its use (Donelan et al. 1985), the problem with spurious correlation is worse with U_c/c_p

TABLE 1. Spurious and physical relations for commonly used dimensionless wave parameters. When the first expression on the right-hand side [for example, $\omega_p (X/g)^{1/2}$ in the first identity] is constant, and at the same time U varies, the dimensionless variables have a functional relation (i.e., all the points fall on the same curve, $\tilde{\omega}_p$ = constant $\cdot \tilde{X}^{-1/2}$ in the first identity).

Spurious relation	Physical relation	Ratio between the exponents
$\tilde{\omega}_p \equiv \omega_p(X/g)^{1/2}\tilde{X}^{-1/2}$	$\tilde{\omega}_p \propto \tilde{X}^{-1/3} \ldots \tilde{X}^{-1/4}$	1.5 . . . 2.0
$\tilde{\epsilon} \equiv \epsilon\omega_p^4/g^2\tilde{\omega}_p^{-4}$	$\tilde{\epsilon} \propto \tilde{\omega}_p^{-4} \ldots \tilde{\omega}_p^{-3}$	1.0 . . . 1.3
$\tilde{\epsilon} \equiv \frac{\epsilon}{X^2}\tilde{X}^2$	$\tilde{\epsilon} \propto \tilde{X} \ldots \tilde{X}^{0.75}$	2.0 . . . 2.7

because U_c is substantially less accurate than U. As Fig. 8 shows, the physical and spurious relations hardly differ at all in this case.

On the other hand, Table 1 shows that the relation between dimensionless energy and dimensionless fetch differs most from the spurious relation. In our analysis, we have therefore put the emphasis on this relation. In the end of section 4c, the effects of spurious correlations in this analysis are examined.

c. *Comparison between experiments*

The analysis revealed that in unstable stratification the growth in Lake Ontario agreed well with the high growth in the Bothnian Sea (Fig. 9). The agreement was remarkably good for the cases of orthogonal fetch when the dimensionless fetch $\tilde{X}$ was shorter than 2000. The datasets begin to separate slightly at longer fetches, and this difference is reflected also in the shape of the spectra. In particular, there are two observations from Lake Ontario at very long dimensionless fetches (out of the range of Fig. 9) that differ greatly from the extrapolation of the short fetch data, possibly because they represent the fully developed stage. We have excluded these two points from our analysis.

In the original analysis of the Lake Ontario data (Donelan et al. 1985), the data in stable and unstable stratification were used together. In addition, some of the differences seems to have been introduced because Donelan et al. derived the energy versus fetch relation with the inverse wave age U_c/c_p as the independent variable, whereas Kahma (1981a) used the dimensionless fetch gX/U^2.

The data from ARSLOE show larger scatter than the other datasets. In addition, only u_* was supplied to the database, and the method used to calculate it seems not to be the same as the method adopted here. Queen Elizabeth II Reservoir data show a change in the slope of the energy versus fetch relation that, as pointed out by Birch and Ewing (1986), is probably related to the strongly slanted fetch. We have therefore excluded these datasets (Fig. 10) from the composite dataset from which the growth equations were determined.

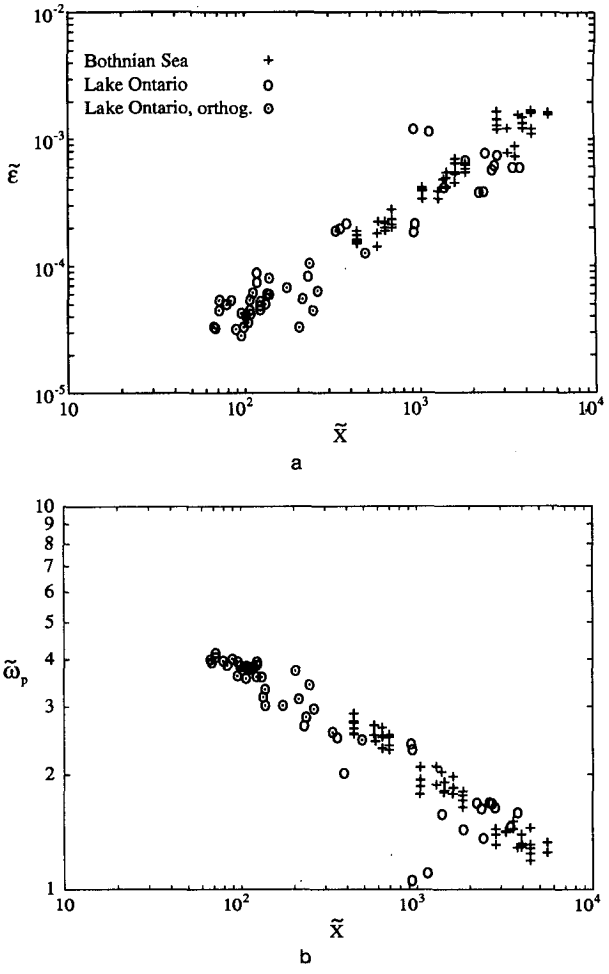

FIG. 9. Dimensionless energy $\tilde{\epsilon}$ and peak frequency $\tilde{\omega}_p$ in the Bothnian Sea data and the Lake Ontario data in unstable stratification.

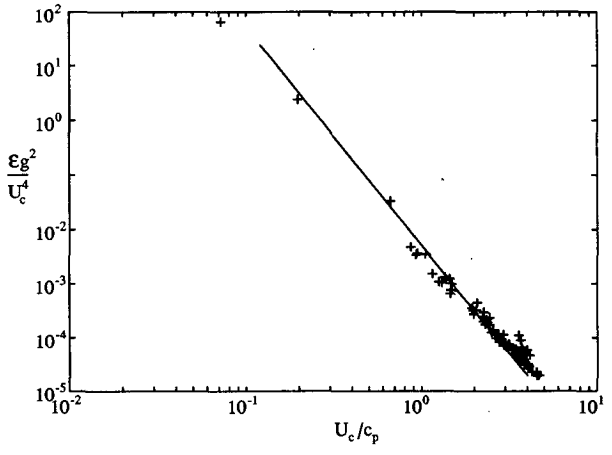

FIG. 8. An illustration of the difficulties to distinguish the physical relation from the spurious relation (the line) when U_c is used for scaling.

The smallest scatter is shown by the stability-stratified Lake Ontario data and, especially, the Bothnian Sea data. These two experiments lasted several months, and it was therefore possible to select events of steady wind. The main JONSWAP experiment, with a large number of wind and wave measuring points, lasted only one month plus a two-week extension with part of the instrumentation. The criteria for the steadiness of the wind could not be so strict, and, as Hasselmann et al. (1973) pointed out, gusts in the wind contribute a great deal to the scatter in the JONSWAP data.

After our other working hypotheses, such as the in-

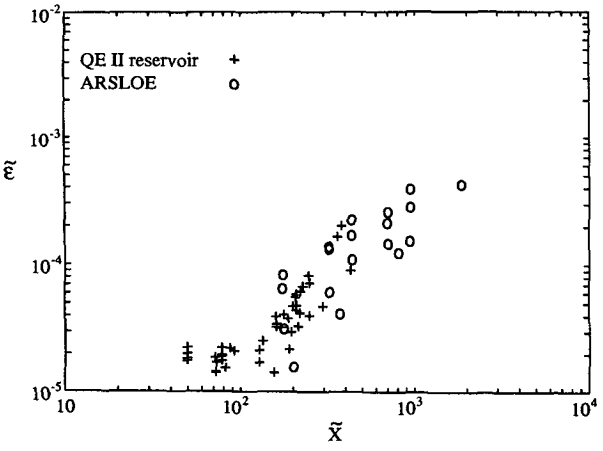

FIG. 10. Dimensionless energy in the ARSLOE data and in the Queen Elizabeth II Reservoir data.

fluence of swell, failed to explain the differences, we decided once more to reanalyze the extensive wind measurements of the JONSWAP experiment. For the reanalysis, the wind data plots were first digitized from the JONSWAP experiment and then an interpolated wind field was calculated from the plots. From this wind field, the wind speed was calculated further at a point moving with the group velocity $c_g = g/2\omega_p$ of the waves at the peak of the spectrum. An example is presented in Fig. 11. This represents the wind felt by the growing waves, and, although the x axis in the figure is shown as fetch, it can equally well be interpreted as time.

The analysis revealed that a number of spectra originally accepted as steady-wind cases were in fact generated in an unsteady or decreasing wind, as the example in Fig. 11 shows. Therefore, the dataset was divided into four groups (Fig. 12): steady wind, increasing wind, decreasing wind, and variable wind. The dimensionless parameters were then calculated using the average wind at a point moving with the waves. The subsets of both increasing wind and steady wind showed considerably less scatter than the subsets of decreasing wind and variable wind. When the new average wind was used and the cases of variable and decreasing wind were excluded, the original scatter in the JONSWAP data (Fig. 13) was substantially reduced (Fig. 14).

Figure 15 shows how the new average wind compares with the wind given in Müller (1976). There are considerable differences between individual data points, but the regression line shows no bias between these two estimates.

The stratification during the JONSWAP experiment was mainly stable. When the JONSWAP data are compared with data from stable stratification in Lake Ontario, we see that they agree well (Fig. 14). We have thus been able to identify two factors that can explain the differences between the three datasets:

1) the influence of atmospheric stratification;
2) variable or decaying wind in some of the originally accepted JONSWAP runs.

This brings up a new question: How comparable were the wind fields in the Bothnian Sea data and the Lake Ontario data on the one hand, and the wind fields of the selected JONSWAP cases on the other? Because the wind measurements during the former two experiments were not as extensive as in JONSWAP, it was not possible to reanalyze their wind speeds by the same method. During the Bothnian Sea experiment and the Lake Ontario experiment, however, the wind in the selected cases had been constant long enough for the wind field to become stationary. It seems therefore likely that, if there is any systematic difference between the wind data available and the wind in the coordinate system moving with the waves, it would be caused only by spatial variations. In the fetch range where the boundary layer is developing we expect that, if the wind is changing, it increases with fetch. Therefore, we can assume that both the Bothnian Sea data and the Lake Ontario data have been measured in a steady or increasing wind, comparable to the selected JONSWAP data in Fig. 14. It is interesting to note that, when the average wind at a point moving with the waves is used, the scatter in the JONSWAP data is comparable to, and at short fetches even smaller than, the Bothnian Sea data and the Lake Ontario data. This once more underlines the importance of detailed information on the wind field.

To be able to compare the datasets numerically with the original JONSWAP relations, equations have been calculated for energy assuming that the growth is linear with fetch. Lake Ontario data in stable stratification contain data from only short fetches, and therefore,

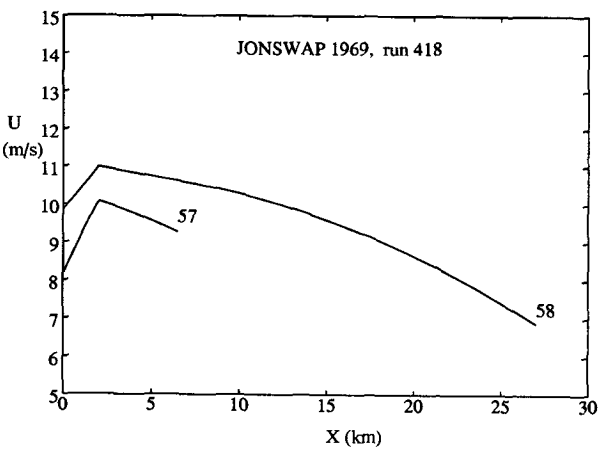

FIG. 11. The time history of U_{10} in run 418 of the JONSWAP experiment at a point moving with the group velocity of the waves at the peak frequency of the wave spectrum. Each line corresponds to the time history of one spectrum (runs 57 and 58 in our database).

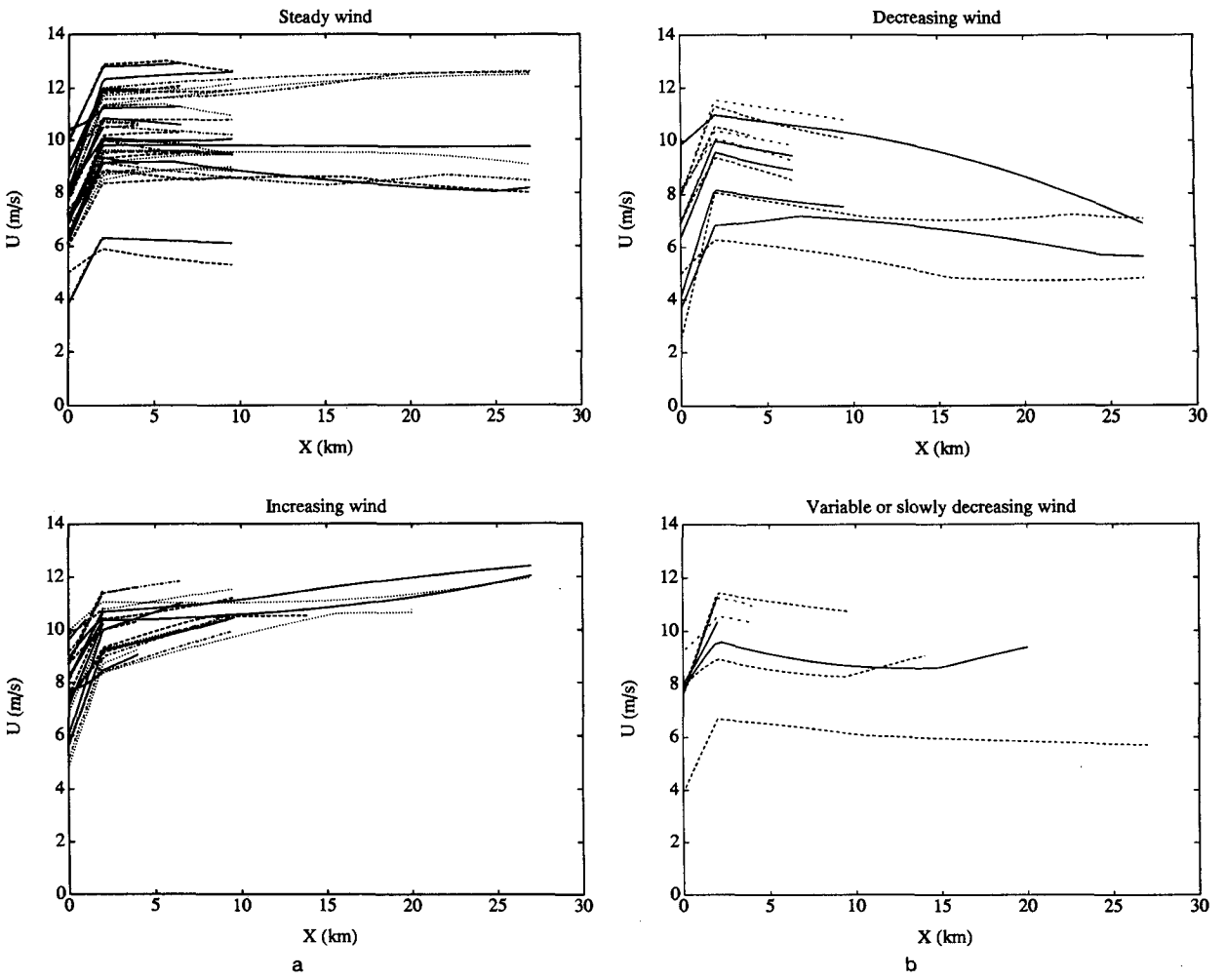

FIG. 12. The time history of U_{10} in the JONSWAP experiment in a coordinate system moving with the group velocity of the waves at the peak frequency of the wave spectrum. The data is divided into groups according to the steadiness.

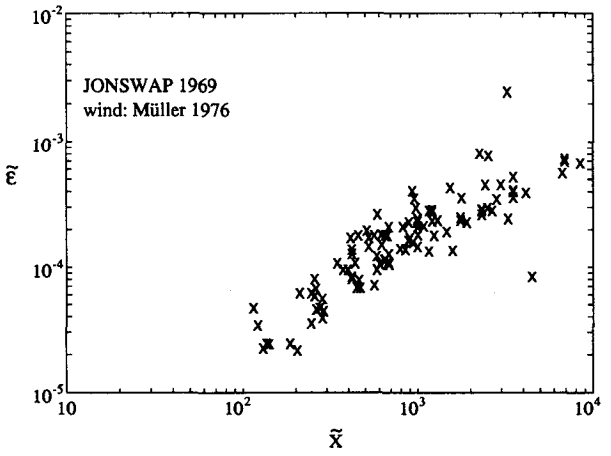

FIG. 13. Dimensionless energy from the JONSWAP dataset using the wind speed given in Müller (1976).

the equations have been calculated for the JONSWAP data for the same short fetch.

Stable stratification	
JONSWAP, Hasselmann et al. 1973	$1.6\ 10^{-7}\tilde{X}$
JONSWAP, this study	$2.1\ 10^{-7}\tilde{X}$
JONSWAP, short fetch $\tilde{X} < 500$,	$2.5\ 10^{-7}\tilde{X}$
Lake Ontario, stable	$2.8\ 10^{-7}\tilde{X}$
Unstable stratification	
Lake Ontario, unstable	$3.8\ 10^{-7}\tilde{X}$
Bothnian Sea	$3.5\ 10^{-7}\tilde{X}$

The present data suggest that in unstable stratification the growth of energy with fetch is fairly close to linear, but in stable stratification the deviation from linear growth seems to be significant. This means that the regression equations cannot be directly compared, and that comparisons using a fixed power law can be misleading.

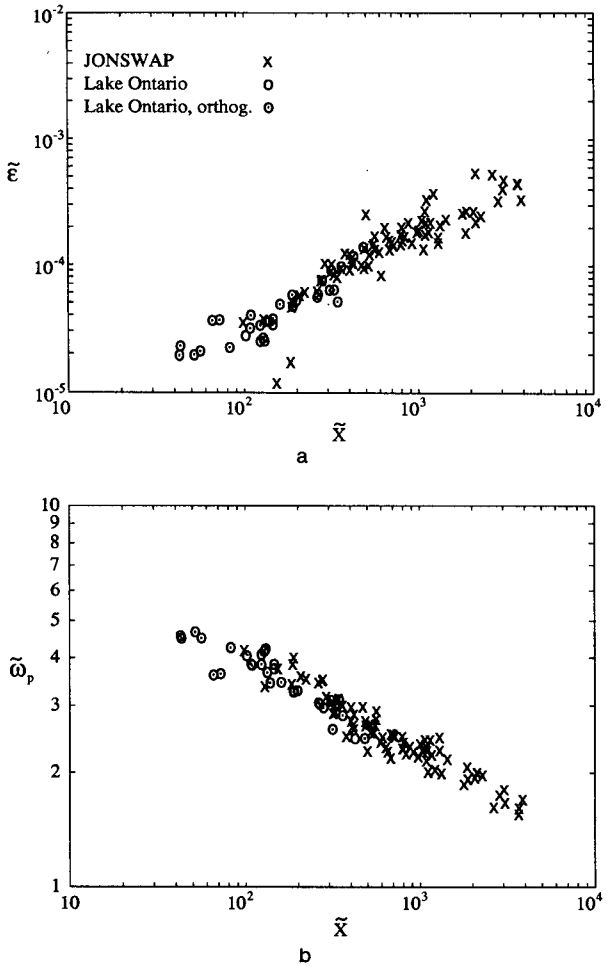

FIG. 14. Dimensionless energy $\tilde{\varepsilon}$ and peak frequency $\tilde{\omega}_p$ in the JONSWAP experiment in steady and increasing wind, scaled by the average wind in the coordinate system moving with the group velocity of the wave at the peak of the spectrum; the same variables in the Lake Ontario experiment in stable stratification.

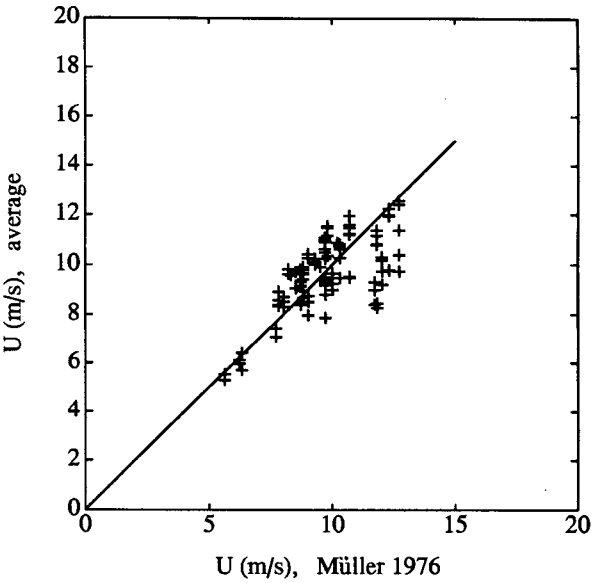

FIG. 15. Comparison of the two wind parameters in the JONSWAP experiment: the wind in the moving coordinate system and the wind given in Müller (1976).

The datasets are therefore compared in pairs. The best-fit power law is first calculated to the composite of the pair and the residuals from this common power law are then compared. To be considered statistically inconsistent, this approach requires that dimensionless energy over the whole dimensionless fetch range of the data is on average different between the groups. A mere difference in the power, if it does not result in a significantly different prediction in energy, will not show up as a statistically significant difference. This is a conservative approach from the point of view of the wave prediction problem, because it will consider only differences that will affect the actual predicted energy.

Between the composite unstable and stable stratification groups the difference is as much as 70%. When only the Lake Ontario data are considered, the difference is somewhat smaller, 48%. Both the differences between stable and unstable groups are statistically highly significant. On the other hand, within the groups of the same stability no statistically significant differences can be found by this approach. Between the stable groups, the difference is 4% and between the unstable groups it is 7%.

The results are similar when the friction velocity is used. The stability correction by Monin–Obukhov similarity theory brings the unstable and stable groups closer together but does not remove all the difference. Between the stable and unstable groups the difference is still 47%. As in the case of U_{10} scaling the difference in Lake Ontario data is smaller than the difference in

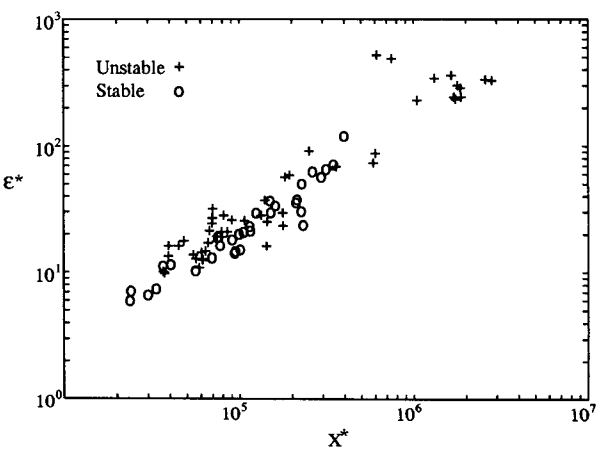

FIG. 16. Dimensionless energy in the Lake Ontario experiment in unstable and stable stratification scaled by u_*.

the composite dataset. But while in Fig. 16 it might look as if in Lake Ontario data the stability difference is essentially removed by friction velocity scaling, the difference is still 23% and it is statistically significant at 98% confidence level. The dataset is sufficiently large that the difference is statistically significant regardless whether the two outliers in Lake Ontario data are included or excluded. Between JONSWAP data and Lake Ontario stable data the difference is 5% and the difference between the Bothnian Sea data and Lake Ontario unstable data is 1%. These differences are not statistically significant.

Some uncertainty results from the fact that in the JONSWAP data the stability parameter z/L is mostly an estimate, because no original temperature data could be found for runs measured in August. E. Bouws, who participated in the JONSWAP field measurements, recalled that during the selected runs, days were warm and there was often fog over the sea, indicating stable stratification. Based on this information and the measurements from June 3 . . . 5°C was used as the air–sea temperature difference for the daytime and near zero for nighttime to calculate rough estimates of z/L.

The uncertainty fortunately is smaller than we originally expected. The difference between unstable and stable groups is 45% if neutral stability is assumed in the JONSWAP data and is still 38% if an unrealistically high air temperature of 30°C is used to replace the missing temperature data in the JONSWAP experiment.

If neutral stability was assumed, scatter could not be reduced by friction velocity scaling. Figures 13, 14, 17, and 18 show how marginally the data points are displaced when u_* is used instead of U_{10}. This should be compared with the great improvement when the average wind at a point moving with the waves is used

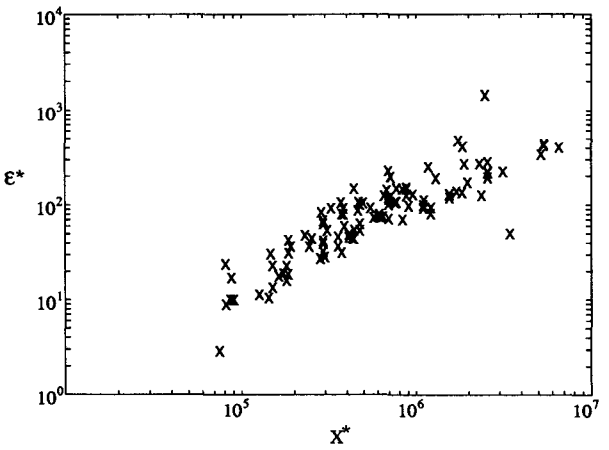

FIG. 17. Dimensionless energy in the JONSWAP experiment scaled by u_* as determined from Müller (1976) with the C_D of Eq. (1).

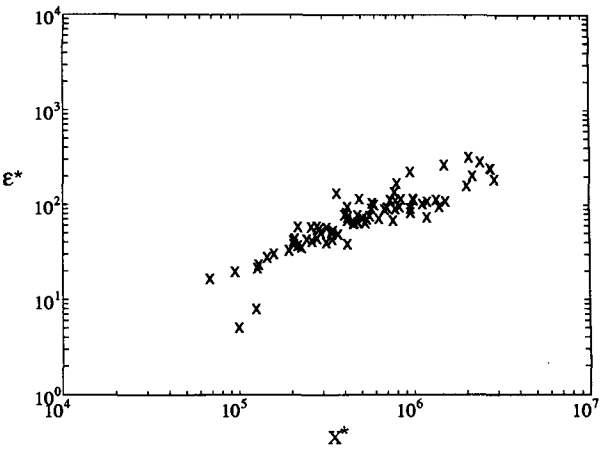

FIG. 18. Dimensionless energy in the JONSWAP experiment using u_* as determined from the moving coordinate average wind with the C_D of Eq. (1).

instead of the average wind calculated by Müller (1976). We want to emphasize, however, that this indicates only that u_* related to the widely used wind-dependent drag coefficient of Eq. (1) gives no advantage over U_{10}. It does not imply that the true friction velocity, if it somehow could be measured or calculated, could not improve the results.

The following table gives the fetch relationships based on the Bothnian Sea, the JONSWAP, and Lake Ontario data. In the aforementioned comparisons we have accepted data points from Lake Ontario in which the fetch is not perfectly orthogonal, because otherwise the overlapping fetch range with JONSWAP data or Bothnian Sea data would have been short. When the relations were calculated the datasets were made as uniform as possible and only orthogonal fetch cases were used. The coefficients are given here to a precision that does not reflect their real accuracy, but which is necessary if one wants to calculate correctly derived equations, such as Eqs. (10) and (11). The coefficients are not significantly affected by the few outliers (JONSWAP and Lake Ontario), the slanting fetch cases (Lake Ontario), or the uncertainty of the stability correction in the JONSWAP data: for example, the maximum change to the power by varying these factors is less than 0.04 and the factor correspondingly changes 6% if the unrealistically high $T_a = 30$°C is used, otherwise only 2%. Because the variables on both axes have uncertainties, the relations were calculated by the maximum likelihood method using the following estimates for the errors: $\tilde{\omega}_p$, 7%; $\tilde{X}$, 10%; and $\tilde{\epsilon}$, 30%.

Stable stratification

$$\tilde{\epsilon} = 9.25 \times 10^{-7} \tilde{X}^{0.766} \tag{2}$$

$$\tilde{\omega}_p = 11.99 \tilde{X}^{-0.242} \tag{3}$$

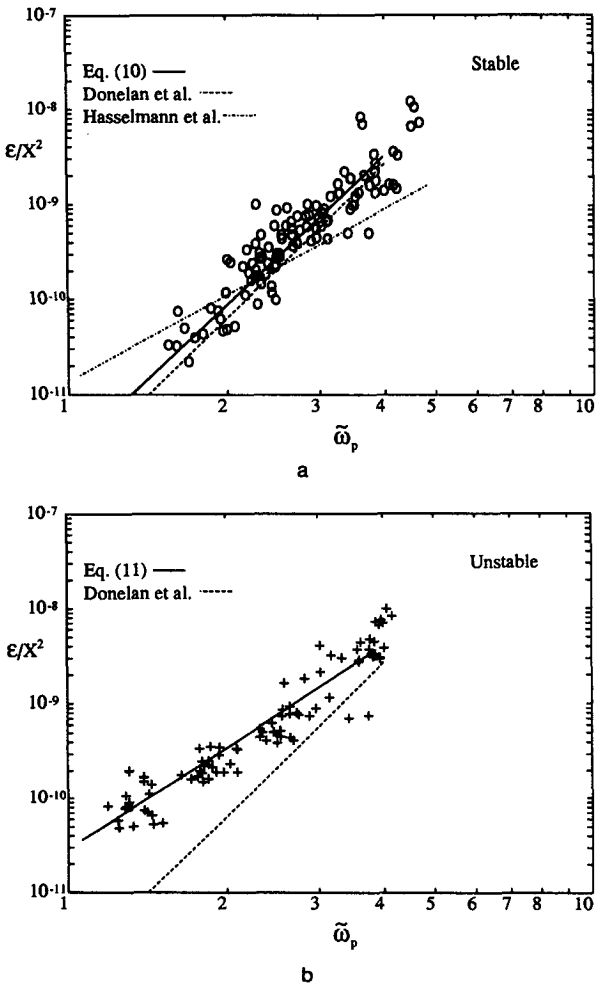

FIG. 19. Relations between the dimensionless parameter ϵ/X^2 and dimensionless peak frequency $\omega_p U/g$. These relations are free from any spurious correlations.

$$\epsilon^* = 2.06 \times 10^{-3} X^{*0.797} \quad (4)$$

$$\omega_p^* = 2.305 X^{*-0.245} \quad (5)$$

Unstable stratification

$$\tilde{\epsilon} = 5.38 \times 10^{-7} \tilde{X}^{0.940} \quad (6)$$

$$\tilde{\omega}_p = 14.19 \tilde{X}^{-0.283} \quad (7)$$

$$\epsilon^* = 4.68 \times 10^{-4} X^{*0.942} \quad (8)$$

$$\omega_p^* = 3.755 X^{*-0.287} \quad (9)$$

We finally discuss the reliability of our estimates from the point of view of spurious correlation.

While the relations in which dimensionless fetch is the independent variable are much less vulnerable than those based on dimensionless frequency (or inverse wave age), spurious correlation is still possible. As a check ϵ/X^2 has therefore been plotted as a function of $\omega_p U/g$. These have no variables in common, and the relation is therefore completely free from any spurious correlation. This relation in itself is not very useful for wave prediction because it assumes that both $\tilde{\omega}_p$ and X are known. We can, however, use it to test the relations between $\tilde{\epsilon}$, $\tilde{\omega}_p$, and $\tilde{X}$ by comparing the data with the relations that follow from Eqs. (2)–(3) and (6)–(7):

$$\text{Stable:} \quad \epsilon/X^2 = 2.7\ 10^{-12} \tilde{\omega}_p^{5.2} \quad (10)$$

$$\text{Unstable:} \quad \epsilon/X^2 = 2.5\ 10^{-11} \tilde{\omega}_p^{3.8}. \quad (11)$$

Figure 19 shows that the data in unstable and stable stratification are very different in these coordinates. The relations (10) and (11) agree well with the data, suggesting that they have not been noticeably corrupted by spurious correlation. On the other hand, the relation of Donelan et al. (1985), while it perfectly describes the relation in stable stratification, very poorly fits the data in unstable stratification (including the data from Lake Ontario in these conditions).

The reason for this can be seen in Fig. 20. It shows the same data in $\tilde{\epsilon} - \tilde{\omega}_p$ coordinates, which correspond closely to the $\tilde{\epsilon}$ and U_c/c_p Donelan et al. (1985) used. In these coordinates the data in unstable and stable stratification differ only marginally, and the continuous line that is the best fit to the composite data happens to lie close to the relation of Donelan et al. (1985).

Surprisingly, in the coordinates of Fig. 19, the original JONSWAP relation (Hasselmann et al. 1973) also deviates from the stable data (again including its own data). This is unexpected, since they used $\tilde{X}$ as the independent variable. The reason could be, as Phillips (1977) suggested, the inclusion of laboratory data in the dataset in Fig. 2.10 of Hasselmann et al. (1973).

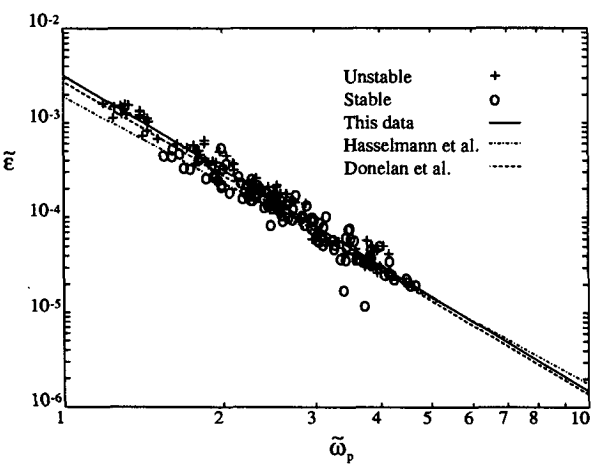

FIG. 20. Dimensionless energy $\tilde{\epsilon}$ versus $\tilde{\omega}_p$ in unstable and stable stratification.

d. Discussion

Many studies in the past have assumed that the stability difference observed in the growth equations comes from the inability of U_{10} to describe the surface stress, and that the stability effect should disappear when friction velocity is used as the scaling wind. Our results contradict this view. In the light of the experimental results concerning the effect of stability on the momentum retained by waves (Donelan 1979) this should, however, have been expected.

The transport equation

$$\frac{\partial S(\omega, \theta)}{\partial t} + c_{gi} \frac{\partial S(\omega, \theta)}{\partial x_i} = G,$$

where $S(\omega, \theta)$ is the directional spectrum, c_g is the group velocity, and G is the source function can be written as a momentum balance equation

$$\frac{\partial}{\partial X}\left[\int\int S(\omega, \theta) \frac{k}{\omega} \frac{d\omega}{dk} \cos^2\theta d\theta d\omega\right] + \frac{\partial}{\partial t}\left[\int\int S(\omega, \theta) \frac{k}{\omega} \cos\theta d\theta d\omega\right] = \frac{\gamma \rho_a u_*^2}{\rho_w g},$$

where $\gamma \rho_a u_*^2$ is the fraction of the total stress τ_a remaining in the waves. In deep water, we may approximate

$$\omega/k = g/\omega$$
$$d\omega/dk = g/2\omega;$$

from this we get for fetch-limited waves

$$\frac{\partial \epsilon}{\partial X} = 2 \frac{\gamma D}{g} \frac{\rho_a}{\rho_w} u_*^2, \tag{12}$$

where D is a function of the directional distribution of the spectrum (e.g., $D = 1$ for long-crested waves, and $D = 4/3$ for the very wide spreading described by $\cos^2\theta$). The factor γD is a slowly varying function of fetch and, as Donelan (1979) has shown, a function of z/L. By definition γ vanishes if the waves are fully developed. For fetch-limited waves γD can be estimated from the fetch relations.

Equation (12) can be rewritten in dimensionless form and integrated to give

$$\epsilon^* = 2 \frac{\rho_a}{\rho_w} \int_0^{X^*} D\gamma dX^* = 2 \frac{\rho_a}{\rho_w} I(X^*, z/L). \tag{13}$$

Now, if u_* is to explain all the variability caused by stability, the integral I should be independent of z/L. Otherwise, the dimensionless energy would change with stability even when X^* remains constant. It is worth noting that, in the special case of γ and D are independent of fetch, we get the linear growth $\epsilon^* = 2(\rho_a/\rho_w)\gamma D X^*$, which shows the point even more clearly.

Equation (13) together with the result that γ, in fact, more than doubles with stability (Donelan 1979) means that scaling by friction velocity cannot explain all the variability arising from stability differences. It is worth noting that Donelan calculated γ using τ_a measured by the correlation method. One could argue that the difference in Fig. 16 results from the imperfections in the model that was used to calculate u_*, but this argument cannot be applied to the γ measured by Donelan.

Air and water densities are so near to constants that they cannot change the above conclusion. It is interesting, however, to note that the density ratio ρ_a/ρ_w may slightly influence the growth curves. It is likely that γ also is affected by the density ratio, but perhaps not exactly inversely. Therefore, it is worth noticing that all these factors (air temperature, water temperature, and salinity) happened to be such that they tended to maximize the difference of the density ratios of the JONSWAP experiment and the Bothnian Sea experiment. The difference turned out to be as high as 10%. Therefore, the pure stability effect could be slightly smaller than the difference between the Bothnian Sea data and the JONSWAP data suggests.

e. Parameterizing the stability effect

The analysis performed so far indicates that there is a significant difference in wave growth in unstable and stable stratification. Only part of it can be removed by using friction velocity scaling, and in other respects the friction velocity calculated using the drag coefficient of Eq. (1) seems to give no advantage over the measured U_{10}.

Comparing the different stability groups suggests that the transitional region between unstable and stable growth is limited to a fairly narrow range near neutral stability. An empirical analysis could be done by studying $\tilde{\epsilon}$ as a function of two dimensionless variables, $\tilde{X}$ and z/L. Unfortunately, the existing data is too scanty for the purpose. The scatter is far too large to reveal anything more than that the growth is faster in unstable than in stable stratification. To parameterize the stability effect, we need assumptions about the mechanism by which it affects wave growth. The models that we are aware of at the moment cannot explain the observed stability effect. For example, using scaling wind speed at height $\lambda/2$ leads to a stability effect opposite to the observed one.

While we feel that the above conclusion is the best that we can at the moment rigorously deduce from the data at our disposal, it is important for practical wave prediction to have a continuous function describing the transition between stable and unstable stratification. To estimate this, we have taken advantage of the fact that the growth curves in these two cases intercept, and roughly at the same dimensionless fetch $\tilde{X}_0$

$\approx 20 \cdots 60$. Furthermore, the dimensionless peak frequency $\tilde{\omega}_p$ at the interception fetch is ≈ 5, which again happens to be close to the dimensionless frequency at which the transition in the grand average (Fig. 7) of the high-frequency tails occurs. For the purpose of parameterizing the stability effect we therefore conjecture that at this frequency the energy and momentum balance change in such a way that the stability is able to affect wave growth only when $\tilde{\omega} < 5$.

Then, the growth equations are rewritten in the following form:

$$\tilde{\epsilon} = \tilde{\epsilon}_0(\tilde{X}/\tilde{X}_0)^{p_\epsilon}, \quad \tilde{\omega}_p = \tilde{\omega}_0(\tilde{X}/\tilde{X}_0)^{p_\omega}.$$

The power p can now be calculated for each data point as a function of the stability parameter z/L. The results are shown in Fig. 21. The points near X_0 naturally show considerable scatter, but the density of the points is now sufficient to fit a function, for which the hyperbolic tangent was chosen. In the case of U_{10} scaling we get (Fig. 21)

$$\tilde{\epsilon} = 10^{-5}(\tilde{X}/23)^{(0.84-0.13\ \tanh(6z/L))} \quad (14)$$

$$\tilde{\omega}_p = 4.4(\tilde{X}/63)^{(-0.26+0.02\ \tanh(6z/L))}, \quad (15)$$

and with u_* scaling (excluding points for which $X^* < 5X_0^*$, Fig. 22)

$$\epsilon^* = 8.1(X^*/31\ 10^3)^{(0.86-0.08\ \tanh(6z/L))} \quad (16)$$

$$\omega_p^* = 0.13(X^*/120\ 10^3)^{(-0.26+0.02\ \tanh(6z/L))}. \quad (17)$$

Because of the uncertainty in the JONSWAP data (cf. section 4c), it is important to verify the result by calculating the exponent p from only the Lake Ontario data. In the case of U_{10} scaling this does not result in any significant change, but in the case of friction velocity scaling the stability effect in the Lake Ontario data is only two thirds of that found in the composite dataset. We assume that the true function would lie somewhere between the two curves in Fig. 22, and we have chosen Eq. (16) accordingly. Our opinion is that the U_{10}-scaled equations are considerably more accurate than the ones scaled by u_*, because less uncertain calculations were involved.

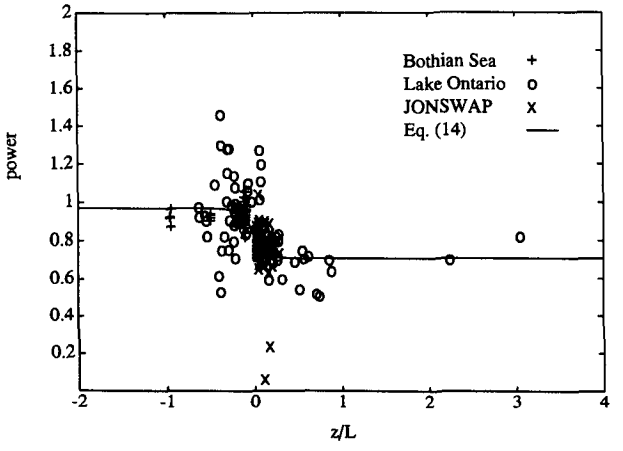

FIG. 21. The power p of the fetch relation $\tilde{\epsilon} = \tilde{X}^p$ as a function of stability.

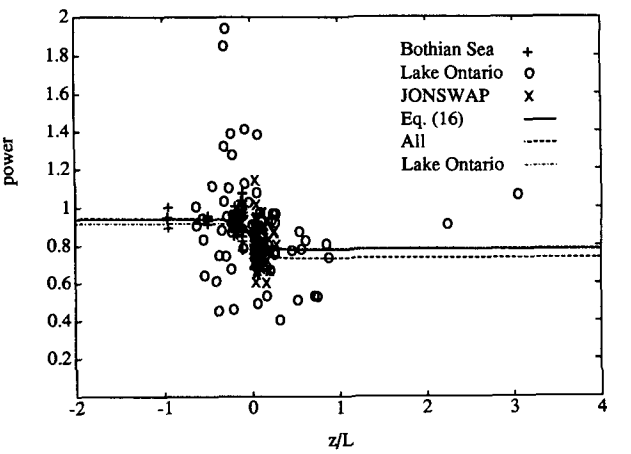

FIG. 22. The power p of the fetch relation $\epsilon^* = X^{*p}$ as a function of stability.

5. The influence of swell

Laboratory experiments have shown that the addition of long mechanical waves dramatically reduces the growth of shorter wind-generated waves. (Mitsuyasu 1966; Phillips and Banner 1974; Hatori et al. 1981; Bliven et al. 1986; Kusaba and Mitsuyasu 1986; Donelan 1987). In these laboratory experiments both the total energy of short waves and the peak enhancement of the spectrum were substantially reduced. In the field it is much more difficult to prove that swell is responsible for the change that can be seen in the peak enhancement. Reduced peak enhancement was found in the Bothnian Sea data when swell arrived in the area after a period of exceptionally steady offshore wind (Fig. 23). The same effect observed in Lake Ontario has been reported by Donelan in the VI WAM meeting in 1988, and by Donelan, Kahma, and Tsanis in the VIII WAM meeting in 1990.

The JONSWAP data contains a number of spectra that were measured in the presence of considerable swell. One of our working hypotheses was, therefore, that this might contribute to the scatter in the JONSWAP data, and to the smaller energy compared with the Bothnian Sea dataset. As Fig. 24 shows, this hypothesis was not confirmed: the energies in the presence of swell were not different from the other measurements. Comparison of the energies in the Bothnian Sea spectra with and without swell gave the same result. These findings do not mean that much steeper swell would not have the effect observed in the laboratory.

6. Conclusions

Our reanalysis confirmed the earlier conclusions on this subject: no single factor seems to be responsible for the large difference between the original JONSWAP wave growth relation and the Bothnian Sea wave growth relation. By reanalyzing the JONSWAP wind data and dividing the Lake Ontario data according to stability, however, we came to the following conclusions:

1) The data from Lake Ontario during unstable stratification show the same rapid growth as the Bothnian Sea data measured in unstable stratification. The growth of energy was approximately linear with fetch in both datasets.

2) The data from Lake Ontario in stable stratification show less rapid growth with fetch than those in unstable stratification and agree with the reanalyzed JONSWAP data, which were measured mainly in stable stratification. The growth of energy with fetch was slower than linear.

3) The effect of stability was partly removed when u_* was calculated using the Monin–Obukhov similarity theory, but otherwise we were not able to improve the results by replacing U_{10} by u_* calculated using the wind-speed–dependent drag coefficient of Eq. (1).

4) The wave prediction relations can be summarized as follows:

Stable stratification

$$\tilde{\epsilon} = 9.3 \times 10^{-7}\, \tilde{X}^{0.76}$$

$$\tilde{\omega}_p = 12.0 \tilde{X}^{-0.24}$$

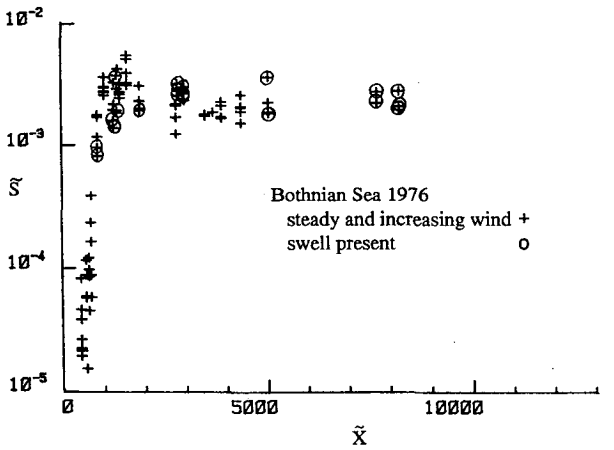

FIG. 23. The dimensionless spectrum $S(\omega)\omega^5/g^2$ at a fixed dimensionless frequency $\omega U/g = 2$ in the Bothnian Sea data (a) during the steady wind period, when the spectra in the dataset were measured, and (b) afterward, when a change in the wind direction at the southern end of the Bothnian Sea brought swell into the study area.

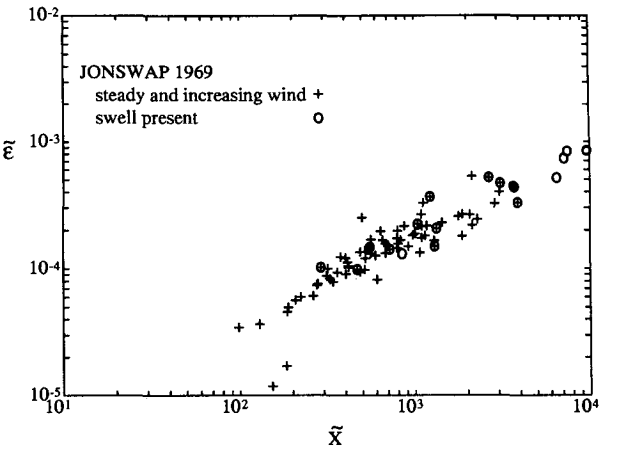

FIG. 24. Dimensionless energy in the JONSWAP experiment in the runs with and without swell.

Unstable stratification

$$\tilde{\epsilon} = 5.4 \times 10^{-7}\, \tilde{X}^{0.94}$$

$$\tilde{\omega}_p = 14.2 \tilde{X}^{-0.28}$$

Composite dataset

$$\tilde{\epsilon} = 5.2 \times 10^{-7}\, \tilde{X}^{0.9}$$

$$\tilde{\omega}_p = 13.7 \tilde{X}^{-0.27}.$$

We estimate that the relations should be valid at least up to dimensionless fetch $\tilde{X} = 8000$ before the effects of the transition to full development become important.

A parameterization of the stability effect is presented in section 4e.

Acknowledgments. We want to thank all the authors and participants of the original experiments who have made their data available to the database. Our special thanks are due to Evert Bouws of KNMI, who provided copies of the complete wind data plots of the JONSWAP experiment and gave us photographs and valuable undocumented details of the experiment.

The work has been carried out at the Delft Hydraulics Laboratory in the Netherlands and at the Finnish Institute of Marine Research. The authors want to thank both institutes for their hospitality during the working visits. The work has been supported by the Natural Sciences Research Council of the Academy of Finland.

REFERENCES

Birch, K. G., and J. A. Ewing, 1986: Observations of wind waves on a reservoir. Institute of Oceanographic Sciences, Rep. No. 234, 34 pp.

Bliven, L. F., N. E. Huang, and S. R. Long, 1986: Experimental study of the influence of wind on Benjamin–Feir sideband instability. *J. Fluid Mech.*, **162,** 237–260.

Bouws, E., 1986: Provisional results of a wind wave experiment in a shallow lake (Lake Marken, The Netherlands). KNMI Afdeling Oceanografisch Onderzoek, Memo 00-86-21, 15 pp.

Charnock, H., 1955: Wind stress on a water surface. *Quart. J. Roy. Meteor. Soc.*, **81,** 639–640.

Donelan, M. A., 1979: On the fraction of wind momentum retained by waves. J. C. J. Nihoul, Ed., *Marine Forecasting,* 141–159.

——, 1987: The effect of swell on the growth of wind-waves. *Symp. on Measuring Ocean Waves from Space,* Baltimore, Johns Hopkins University.

——, and W. J. Pierson, 1987: Radar scattering and equilibrium ranges in wind-generated waves with application to scatterometry. *J. Geophys. Res.*, **92**(C5), 4971–5029.

——, J. Hamilton, and W. H. Hui, 1985: Directional spectra of wind-generated waves. *Phil. Trans. R. Soc. Lond.*, **A315,** 509–562.

Forristall, G. Z., 1981: Measurements of saturated range in ocean wave spectra. *J. Geophys. Res.*, **86,** 8075–8089.

Hasselmann, K., T. P. Barnett, E. Bouws, H. Carlson, D. E. Cartwright, K. Enke, J. A. Ewing, H. Gienapp, D. E. Hasselmann, P. Kruseman, A. Meerburg, P. Müller, D. L. Olbers, K. Richter, W. Sell, and H. Walden, 1973: Measurements of wind-wave growth and swell decay during the Joint North Sea Wave Project (JONSWAP). *Dtsch. Hydrogr. Z.*, **12,** 1–95.

Hatori, M., M. Tokuda, and Y. Toba, 1981: Experimental study on strong interactions between regular waves and wind waves. *J. Ocean. Soc. Japan,* **37,** 111–119.

——, D. B. Ross, P. Müller, and W. Sell, 1976: A parametric wave prediction model. *J. Phys. Oceanogr.*, **6,** 200–228.

Janssen, P. A. E. M., G. J. Komen, and W. J. P. de Voogt, 1984: An operational coupled hybrid wave prediction model. *J. Geophys. Res.*, **89,** 3635–3654.

——, ——, and ——, 1987: Friction velocity scaling in wind-wave generation. *Bound.-Layer Meteor.*, **38,** 29–35.

Kahma, K. K., 1981a: A study of the growth of the wave spectrum with fetch. *J. Phys. Oceanogr.*, **11,** 1503–1515.

——, 1981b: On the wind speed dependence of the saturation range of the wave spectrum. M. Leppäranta, Ed., *X geofysiikan päivät Helsingissä,* 23.–24.4, 61–67.

——, 1986: On prediction of the fetch-limited wave spectrum in a steady wind. *Finn. Mar. Res.*, **253,** 52–78.

Kitaigorodskii, S. A., 1962: Applications of the theory of similarity to the analysis of wind-generated wave motion as a stochastic process. Izv. Akad. Nauk SSSR, *Geophys. Ser.*, **1,** 105–117.

——, 1970: The Physics of Air–Sea Interaction. English ed., 237 pp.

——, 1983: On the theory of the equilibrium range in the spectrum of wind-generated gravity waves. *J. Phys. Oceanogr.*, **13,** 816–827.

Kusaba, T., and H. Mitsuyasu, 1986: Nonlinear instability and evolution of steep water waves under wind action. *Rep. Inst. Appl. Mech.*, **33**(101), 33–64.

Liu, P. C., and D. B. Ross, 1980: Airborne measurements of wave growth for stable and unstable atmospheres in Lake Michigan. *J. Phys. Oceanogr.*, **10,** 1842–1853.

Lo, A. K., and G. A. McBean, 1978: On the relative errors in methods of flux calculations. *J. Appl. Meteor.*, **17,** 1704–1711.

Mitsuyasu, H., 1966: Interactions between water waves and wind (1). *Rep. Inst. Appl. Mech.*, **14,** 67–88.

Monin, A. S., and A. M. Yaglom, 1971: *Statistical Fluid Mechanics.* The MIT Press, 769 pp.

Müller, P., 1976: Parameterization of one-dimensional wind wave spectra and their dependence on the state of development. Hamburger Geophysikalishe Einzelschriften, Heft 31, 177 pp.

Phillips, O. M., 1977: *The Dynamics of the Upper Ocean,* 2d ed. Cambridge University Press, 336 pp.

——, and M. L. Banner, 1974: Wave breaking in the presence of wind drift and swell. *J. Fluid Mech.*, **66,** 625–640.

Rottier, J. R., and C. L. Vincent, 1982: Fetch limited wave growth observed during ARSLOE. Oceans 82.

The SWAMP Group, 1985: *Ocean Wave Modeling.* Plenum Press, 256 pp.